Journal of materials and Environmental Sciences
ISSN : 2028-2508

JMES, 2017 Volume 8, Issue 2, Page 444-456

http://www.jmaterenvironsci.com/

Spectroscopic and structural studies of nano-sized bioactive materials based on metal mercaptotriazole assemblies

D. M. Fouad,[1] A. M. Hammam (the late), M. A. El-Gahami,[1,2] Z. A. Khafagy,[1]
M. S. Al-Salimi[1] and S. A. Ibrahim[1]*
[1]Chemistry Department, Faculty of Science, Assiut University, Assiut, Egypt; [2]Jeddah University, KSA.

Received 09 Nov 2016,
Revised 14 Dec 2016,
Accepted 15 Dec 2016

Keywords

- ✓ Ternary complexes,
- ✓ Nano-sized,
- ✓ Bioactive,
- ✓ Mercaptotriazoles,
- ✓ Thermodynamics

Saidibrahim7@yahoo.com

Abstract

New nano-sized materials involving some transition metal ions and mercaptotriazoles as well as dithiocabamate or 8-hydroxyquinoline have been prepared. A number of experimental techniques has been used for characterization and structure elucidation of these mixed ligand complexes including elemental analysis, spectroscopic measurements (FT-IR, UV-Vis.), molar conductance, magnetic measurements, X-ray powder diffraction (XRD), transmission electron microscopy (TEM) and thermal studies. Both XRD and TEM measurements provided a clear indication of the nano-sized morphology of the prepared materials. The complexes are hexacoordinate, their structure is thus octahedral and the stoichiometric ratios of these complexes are [M:L:L$'$]= 1:1:1 or 1:1:2 (where L= L_1, L_2 or L_3, L$'$= dtc or quin). Coordination takes place through the sulfur and nitrogen atoms for triazole ligands, two sulfur atoms in case of dtc and through both nitrogen and oxygen atoms in case of quinoline ligand. The thermal decomposition study of the complexes was monitored by TG, DTG and DTA analysis in dynamic nitrogen atmosphere. Thermal studies confirmed the chemical formulations of these complexes. The kinetic parameters were determined from the thermal decomposition data using the graphical methods of Coats-Redfern and Horwitz-Metzger. Thermodynamic parameters were computed using standard relations. Enhanced bioactivity against bacteria has been observed for the tested nano-sized ternary complexes relative to their binary analogs.

1-Introduction

The wide applications of the triazole, dithiocarbamate, quinoline ligands and their metal complexes in biological, pharmaceutical and industrial fields motivated us to study the possibility of preparing nanoparticles including their transition metal ions assemblies. For example, gold (III) dithiocarbamate complexes have been prepared and used for treatment of human cancer to suppress tumor growth via direct inhibition of the protein[1], on the other hand, dithiocarbamate ligands have practical applications in agriculture and for treatment of alcoholism [2,3]. The dithiocarbamate species ($RR\text{-}NCS_2^-$) form an important family of classical anionic ligands. These anions are 3-electron donors, capable of stabilizing metal centers in a variety of oxidation states [4]. 8-Hydroxyquinoline (quin) and its derivatives as well as related metal complexes play a uniquely important role in different disciplines of chemical research and applications [5]. For example, quin was an excellent reagent for the extraction of metal ions and is applied for separation techniques and analytical purposes due to its unique coordinating capabilities[6–9]. In recent years, great attention has been focused on the transition metal complexes with heterocyclic ligands containing thioamide group (-HN-C=S ↔ -N=C-SH) due to their structural features and also because of their biological importance[10-17]. In the present work, we report the preparation and characterization of some new nano-sized materials based on the reaction of transition metals with 4-substituted-amino-3-mercapto-5-benzayl-1,2,4-triazoles, in which the ligand coordinates bidentately with the metal ion through both sulfur and nitrogen atoms as well as adding(dtc) and(quin) as secondary ligands forming mixed ligand complexes with coordination occurring through sulfur, nitrogen and oxygen donor atoms. The so obtained ternary complexes were tested for their antimicrobial activity.

2. Experimental

2.1. *Synthesis of the 4-Substituted-amino-3-Mercapto-5-Benzayl-1,2,4-Triazoles Ligands*

The ligands 4-(2-pyridylmethylenamino)-3-mercapto-5-benzyl-1,2,4-triazole (L_1), 4-(3-pyridylmethylenamino)-3-mercapto-5-benzyl-1,2,4-triazole(L_2), 4-(4-pyridyl methylen-amino)-3-mercapto-5-benzyl-1,2,4-triazole (L_3) were synthesized according to the literatures procedures [18-26].The structures of ligands are shown in Scheme 1.

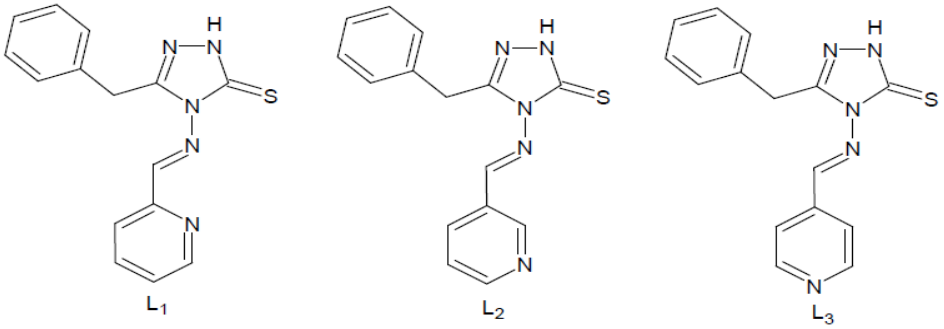

Scheme 1: Structure of the ligands

2.2. Synthesis of Cu(II), Ni(II), Co(II) and Cd(II) Mixed Ligand Complexes

To 1 mmol of $CuCl_2·2H_2O$, $NiCl_2.6H_2O$, $CoCl_2.6H_2O$ or $CdCl_2.2.5H_2O$ solution in 10 mL hot ethanol, a hot ethanolic solution of L_1, L_2 or L_3 (1 mmol in 40 mL) was added dropwise with constant stirring in one direction. When the precipitate was formed, 1mmol in 10 mL hot ethanolic of dtc or quin was added. The pH was adjusted to 7.2–8.2 using dilute ammonia solution. The resulting solution was refluxed for 8 hours. The precipitate obtained was left overnight, filtered through sintered glass, washed with cold ethanol and dried in vacuum over P_4O_{10}.

2.3. Physical Measurements

The carbon, hydrogen, nitrogen and sulfur contents of the solid complexes were determined by elemental analyzer system Gmbh Vario El. Conductivity measurements for the various complexes were carried out using Jenway 4320 meterlab conductivity meter in DMF solutions at 10^{-3} M concentrations at room temperature. Electronic spectra of the solid complex DMF solutions were run on a Perkin Elmer Lambda 40 UV/VIS spectrophotometer using 1-cm matched silica cells. Magnetic susceptibility measurements were carried out at room temperature using a magnetic susceptibility balance of the type MSB-Mk1. Molar susceptibilities were corrected for diamagnetism of the component atoms by the use of Pascal’s constants. The infrared spectra (FTIR) of the free ligands and their metal complexes were recorded on a Shimadzu 470 infrared spectrophotometer (4000-400 cm^{-1}) using KBr discs. Thermal studies of the various complexes were carried out using a Shimadzu DTG-60Hz thermal analyzer, at a heating rate 10 $^{o}C\ min^{-1}$ in dynamic nitrogen atmosphere. Transmission electron microscopy was used to measure the particle size. TEM pictures were taken using a JEOL transmission microscope (model JEM100CX11) with an acceleration voltage of 80kV. X-ray diffraction (XRD) measurements were carried out using Cu-Kα radiation (λ= 0.1541 nm) operated at 40 kV and 40 mA (type PW 1710 control unit Philips) and graphs were plotted using Origin software.

2.4 Antimicrobial activity of the mixed ligands complexes

The antimicrobial activity of the mixed ligand complexes was tested against six bacterial strains. All microbial strains were kindly provided by the Assiut University Mycological Center (AUMC). Measurements have been done using the same method as reported in our previous study[26].

3. Results and discussion

3.1. Elemental Analyses and Conductivity Measurements

All the prepared materials are solids, non-hygroscopic and insoluble in common organic solvents. However, they are soluble in polar solvents such as DMF and DMSO. The molar conductance values fall in the 6.1 – 41.2 $Ohm^{-1}\ cm^2\ mol^{-1}$ range which suggests the non-electrolytic nature of the complexes (Table 1). Some complexes showed molar conductance values within the range 68.4 – 86.3 $Ohm^{-1}\ cm^2\ mol^{-1}$ indicating that these complexes are 1:1 electrolytes [27]. The analytical data of the metal complexes reported in Table1 reveal the formation of complexes having 1:1:1and 1:1:2 (metal ion: triazole ligand: dtc or quin) ratio with Cu(II), Ni(II), Co(II)and Cd(II)ions.

Table 1: Analytical and physical data for the mixed ligand complexes

No.	Complexes [Empirical formula] (Formula weight)	Colour	Analytical Data %Found (Calculated)				Λ_m^* $Ohm^{-1}cm^{2}mol^{-1}$	μ_{eff} B.M.
			C	H	N	S		
1	$[Cu(L_1)(dtc)_2].3H_2O$ $CuC_{25}H_{39}N_7S_5O_3$ M.wt = 708.12	brown	42.12 (42.36)	5.76 (5.55)	13.36 (13.84)	21.94 (22.57)	41.2	2.41
2	$[Cu(L_2)(dtc)(H_2O)Cl].0.5H_2O$ $CuClC_{20}H_{26}N_6S_3O_{1.5}$ M.wt = 568.03	green	41.82 (42.25)	4.18 (4.61)	14.46 (14.79)	16.05 (16.88)	30.0	2.35
3	$[Cu(L_3)(dtc)(H_2O)_2]Cl.2.5H_2O$ $CuClC_{20}H_{32}N_6S_3O_{4.5}$ M.wt. = 622.06	green	38.81 (38.58)	5.12 (5.18)	13.01 (13.50)	15.57 (15.41)	68.4	2.32
4	$[Ni(L_1)(dtc)(H_2O)Cl].H_2O$ $NiClC_{20}H_{27}N_6S_3O_2$ M.wt. = 572.02	yellow	41.71 (41.95)	4.89 (4.75)	14.41 (14.68)	16.98 (16.76)	24.0	3.12
5	$[Ni(L_2)(dtc)(H_2O)Cl].0.5\ H_2O$ $NiClC_{20}H_{26}N_6S_3O_{1.5}$ M.wt. = 563.03	yellow	42.00 (42.62)	4.79 (4.65)	14.32 (14.92)	17.10 (17.03)	15.3	2.91
6	$[Ni(L_3)(dtc)(H_2O)Cl]$ $NiClC_{20}H_{25}N_6S_3O$ M.wt. = 554.02	green	43.45 (43.31)	4.52 (4.54)	15.38 (15.16)	16.83 (17.31)	20.0	2.76
7	$[Co(L_1)(dtc)(H_2O)_2]Cl$ $CoClC_{20}H_{27}N_6S_3O_2$ M.wt. = 573.03	brown	41.28 (41.88)	4.12 (4.74)	14.37 (14.66)	15.77 (16.73)	86.3	4.51
8	$[Co(L_2)(dtc)(H_2O)Cl]$ $CoClC_{20}H_{25}N_6S_3O$ M.wt. = 555.02	brown	43.53 (43..24)	4.73 (4.53)	15.55 (15.13)	17.04 (17.28)	6.1	4.91
9	$[Co(L_3)(dtc)(H_2O)Cl]$ $CoClC_{20}H_{25}N_6S_3O$ M.wt. = 555.02	brown	43.52 (43.24)	4.92 (4.53)	14.86 (15.13)	17.27 (17.28)	13.4	5.12
10	$[Cd\ (L_1)(dtc)(H_2O)Cl]$ $CdClC_{20}H_{25}N_6S_3O$ M.wt. = 610.03	white	39.82 (39.34)	3.96 (4.09)	12.44 (13.77)	14.25 (15.73)	6.8	-
11	$[Cd(L_2)(dtc)(H_2O)Cl].2H_2O$ $CdClC_{20}H_{29}N_6S_3O_3$ M.wt. = 646.02	white	36.83 (37.15)	4.28 (4.52)	12.91 (13.00)	14.32 (14.84)	9.0	-
12	$[Cd(L_3)(dtc)(H_2O)_2]Cl.2H_2O$ $CdClC_{20}H_{31}N_6S_3O_4$ M.wt. = 664.02	white	36.12 (36.14)	4.92 (4.70)	12.38 (12.65)	14.89 (14.44)	71.1	-
13	$[Cu(L_3)(quin)(H_2O)Cl].0.5H_2O$ $CuClC_{24}H_{22}N_6SO_{2.5}$ M.wt. =564.04	brown	51.99 (51.05)	4.15 (3.93)	14.55 (14.89)	5.15 (5.66)	26.5	2.38
14	$[Ni(L_1)(quin)(H_2O)_2]Cl.H_2O$ $NiClC_{24}H_{25}N_6SO_4$ M.wt. =586.06	green	49.66 (49.14)	4.02 (4.29)	14.64 (14.33)	5.5 (5.45)	82.6	3.42
15	$[Ni(L_2)(quin)(H_2O)Cl].0.5H_2O$ $NiClC_{24}H_{22}N_6SO_{2.5}$ M.wt. = 559.05	green	51.52 (51.51)	3.53 (3.96)	15.44 (15.02)	5.78 (5.72)	37.4	3.35
16	$[Co(L_2)(quin)(H_2O)Cl]$ $CoClC_{24}H_{21}N_6SO_2$ M.wt. = 551.05	brown	52.90 (52.26)	3.68 (3.84)	14.96 (15.24)	5.41 (5.80)	35.2	4.92
17	$[Co(L_3)(quin)(H_2O)Cl]$ $CoClC_{24}H_{21}N_6SO_2$ M.wt. = 551.05	brown	52.04 (52.26)	3.46 (3.84)	14.28 (15.24)	4.94 (5.80)	26.7	5.25
18	$[Cd(L_1)(quin)(H_2O)_2]Cl$ $CdClC_{24}H_{23}N_6SO_3$ M.wt. = 624.02	white	46.21 (46.15)	3.03 (3.71)	13.43 (13.46)	5.78 (5.12)	76.4	-

3.2.FTIR Spectra

Relevant IR bands that provide considerable structural evidence for the formation of mixed ligand complexes are reported in Tables 2 and 3. The assignment of the bands due to the -CS_2 moiety has caused great controversy in the literature. Usually, two bands, close to 985 and 625 cm^{-1} have been assigned to the stretching vibrations of this group. However, some authors [28,29] have assigned these bands to carbon-sulfur vibrations in the C=S and C-S groups, respectively. Further confirmation of this assumption comes from the X-ray photoelectron spectra of these compounds, indicating that the equivalence between both sulfur atoms [30]. These bands suffer a shift to higher frequencies in the mixed ligand complexes.

Table 2: IR bands (cm^{-1}) of the mixed ligand (dtc) complexes.

				Thioamide bands				**dtc characteristic bands**			
				I	**II**	**III**	**IV**			**υ(C=S)**	
No.	**υ(H_2O)**	**υ(N–H)**	**υ(C=N)**	**δ(C-H) δ(N-H)**	**υ(C-H) υ(C=S) δ(C-N)**	**υ(C-N) υ(C-S)**	**υ(C=S)**	**υ(C-N) $[NCS_2]^-$**	**υ(N-C) (CNC)**	**υ_{asym} (C-S)**	**υ_{sym} (C-S)**
dtc	3360	-	-	-	-	-	-	1470	1128	985	625
1	3411	3022	1629	1522	1345	1060	852	1490	1142	995	689
2	3418	3045	1623	1582	1325	1023	814	1484	1155	998	691
3	3325	3141	1614	1513	1342	1074	836	1445	1152	990	689
4	3370	3138	1631	1524	1340	1070	838	1514	1140	990	689
5	3346	3125	1619	1521	1353	1073	843	1521	1154	988	690
6	3422	3055	1616	1570	1344	1084	851	1523	1156	988	690
7	3414	3010	1637	1561	1336	1066	853	1480	1135	996	682
8	3394	3005	1618	1551	1350	1070	850	1494	1135	992	688
9	3367	3040	1617	1557	1352	1073	821	1490	1136	989	692
10	3316	3022	1630	1431	1372	1070	834	1495	1151	993	696
11	3450	3024	1615	1570	1356	1071	827	1488	1137	995	690
12	3457	3011	1613	1525	1358	1060	823	1494	1130	990	687

There are three bands observed in the IR spectrum of (quin) ligand corresponding to the frequencies of υ(OH), υ($C_{(aryl)}$-O) and υ(C=N) modes(Table 3). The υ(OH) occurs at around 3380 cm^{-1} as a broad band which is assigned due to the presence of intramolecular H-bonding interactions involving the O-H···N bonds. So the H-bonded OH groups have been replaced by the metal ion. These observations support the formation of M-O bonds via deprotonation [31]. Two other bands are observed in the spectrum of the free (quin) ligand at 1620 and 1155 cm^{-1} which are assigned to υ(C=N) and υ($C_{(aryl)}$-O) vibrations, respectively [31]. The υ(OH) band is absent in the synthesized complexes, while the strong band at around 1155 cm^{-1} due to υ($C_{(aryl)}$-O) in the ligand is shifted to higher frequency in its complexes confirming the bonding of metal ion to the ligand through the oxygen atom [31-34]. L_1, L_2 and L_3 ligands show four bands at 1520–1588 cm^{-1}, 1300–1400 cm^{-1}, 1008–1040 cm^{-1} and 700-850 cm^{-1} which are assignable to thioamide I, II, III, IV vibrations, respectively [19, 35]. These bands have contributions from δ(C-H) + δ(N-H), υ(C=S) + υ(C-N) + δ(C-H), υ(C-N) + υ(C-S) and υ(C=S) modes of vibrations, respectively. These bands will suffer different shifts (e.g. blue or red shift) depending on the modes of coordination to the metal ions. In the complexes, these bands shift to a lower frequency suggesting the coordination of the sulfur atom to the metal ions. [19, 36]. The υ(C=N) vibrations of the azomethine group appear in the region 1613-1637 cm^{-1} in the IR spectra of the obtained mixed ligand complexes, This band is shifted to higher wavenumbers indicating that the azomethine nitrogen atom is coordinated to the metal ion [37]. The presence of coordinated water in the complexes [19, 38] is indicated by a broad band in the region 3316 – 3457 cm^{-1} and two weaker bands in the region 800–750 and 600 – 625 cm^{-1} due to υ(OH), rocking and wagging modes of vibration, respectively [19, 39].

Table 3: IR bands (cm^{-1}) of the mixed ligand (quin) complexes.

			quin characteristic bands		Thioamide bands			
					I	II	III	IV
No.	υ(OH)	υ(N–H)	υ(C-O)	υ(C=N)	δ(C-H) δ(N-H)	υ(C-H) υ(C=S) δ(C-N)	υ(C-N) υ(C-S)	υ(C=S)
quin	3380	3150	1155	1620	-	-	-	-
13	3426	3056	1233	1585	1498	1272	1026	810
14	3365	3035	1265	1600	1511	1250	1046	810
15	3340	3043	1246	1605	1500	1272	1022	805
16	3435	3050	1155	1595	1500	1260	1020	813
17	3382	3045	1260	1594	1495	1262	1015	800
18	3450	3044	1250	1609	1498	1294	1005	821

3.3. Electronic Spectra and Magnetic Measurements

The electronic spectra of the mixed ligand complexes have been recorded in DMF solutions (1×10^{-3} and 1×10^{-4} M, e.g. Fig.1) in the wavelength range 200-1100 nm. The υ_{max} (kK) and ε_{max} (cm^2 mol^{-1}) are depicted in Table 4. The corrected magnetic susceptibilities (μ_{eff}) in Bohr magneton units of the mixed ligand complexes are given in Table 1. The first set of the electronic spectral bands with υ_{max} in the range 30.67 – 37.31 kK, could be attributed to intraligand charge transfer transitions. The second set includes bands having υ_{max} in the range 20.32 – 29.23 kK. These bands are assigned to be LMCT transitions [40]. The third set of bands of Cu(II) complexes 1 – 3 and 13 (Table 4) was found to have υ_{max} within the range 15.50 – 16.94 kK. These bands are due to d-d transitions which are typical for distorted octahedral Cu(II) complexes [19, 41]. These bands could be assigned to include all the three transitions $^{2}B_{lg}\rightarrow{}^{2}B_{2g}$, $^{2}B_{lg}\rightarrow{}^{2}A_{lg}$ and $^{2}B_{1g}\rightarrow{}^{2}E_{g}$ [19]. The magnetic moment values for Cu(II) mixed ligand complexes 1-3 and 13 at room temperature were found to be within the range 2.32 – 2.41 B.M. (Table 1). These values are typical with those expected for tetragonally distorted octahedral Cu(II) complexes [42-44]. the d-d band of Ni(II) mixed ligand complexes 4 - 6, 14 and 15were found to have υ_{max} within the range 15.62-15.81kK. This band could be assigned to $^{3}A_{2g}(F)\rightarrow{}^{3}T_{1g}(F)$ transition, suggesting an octahedral geometry [19, 45]. The magnetic moment for the Ni(II) mixed ligand complexes at room temperature were found in the range 2.76 - 3.42 B.M.(Table 1)which are consistent with their octahedral structure [19, 42]. The electronic spectra of Co(II) complexes (Table 4) exhibited a doublet absorption band with two peaks in the region of 15.15– 15.57 kK and 16.23 – 16.52 kK, corresponding to υ_2 and υ_3 transitions respectively, which are attributed to the transitions $^{4}T_{lg}(F)\rightarrow{}^{4}A_{2g}(\upsilon_2)$ and $^{4}T_{lg}(F)\rightarrow{}^{4}T_{lg}(P)(\upsilon_3)$ [19, 46,47]. These bands are typically characteristic of high spin octahedral Co(II) complexes. These complexes showed a magnetic moment (μ_{eff}) of 4.51 – 5.25 B.M., within the expected range of the octahedral complex 4.3–5.2 B.M. [19, 42, 44]. Cd (II) complexes are diamagnetic and colorless as expected for d^{10} system. On the basis of elemental analysis, infrared spectra, molar conductance value and thermal analysis, octahedral geometry can be suggested for these Cd (II) complexes.

3.4. XRD and transmission electron microscopy (TEM)

X-ray powder diffraction together with the electron microscopy images have been used to check the nano-sized characteristics of the prepared materials. Transmission electron microscopy, TEM, was used to determine the particle size of the prepared complexes. TEM allows the direct imaging of nanoparticles and provides more information on the quality of individual particles, e.g. their size, distribution and shape [48]. The TEM image of complex $[Ni(L_3)(dtc)(H_2O)Cl]$ (Fig.2) shows the formation of nanoparticles aggregates. The size of the nanoparticles that form the aggregates ranged from 38.2 and 69.6 nm with a mean particle size of 49.1 nm (Fig.2). The X-ray diffraction pattern of the complex $[Ni(L_3)(dtc)(H_2O)Cl]$ is shown in Fig.3. The lattice parameters are determined with the aid of CRYSFIRE computer program [49]. The relative broadening of the peaks indicates that the particles are small in size. The values of interplanar spacing, d, and Miller indices, hkl, for each diffraction peak before and after refinement are determined by using CHEKCELL program [49]. The values of d and corresponding hkl and the results show that this complex has orthorhombic crystal structure with space group PMC21. The lattice parameters are estimated to be: a = 10.62 Å, b = 6.49 Å, c = 7.97 Å, $\alpha = \gamma = 90$ and $\beta = 90.06$.

Table 4: Electronic spectral data of the mixed ligand complexes (1×10^{-3} and 1×10^{-4} M in DMF solutions).

No.	complexes	υ_{max}(kK) (ϵ_{max}cm^2 mol^{-1})	Assignment
1	$[Cu(L_1)(dtc)_2].3H_2O$	36.76(19976) 32.46(10689) 26.31(2000) 16.07(1667)	intraligand intraligand LMCT d – d
2	$[Cu(L_2)(dtc)(H_2O)Cl].0.5H_2O$	35.46(11663) 31.74(8889) 25.31(1909) 16.94(154.08)	intraligand intraligand LMCT d – d
3	$[Cu(L_3)(dtc)(H_2O)_2]Cl.2.5H_2O$	35.08(9927) 32.36(8763) 16.00(568.8)	intraligand intraligand d – d
4	$[Ni(L_1)(dtc)(H_2O)Cl].H_2O$	35.46(8440.8) 20.32(98.35) 15.77(32.983)	intraligand LMCT d – d
5	$[Ni(L_2)(dtc)(H_2O)Cl].0.5\ H_2O$	35.71(50365) 20.83(163.647) 15.62(57.694)	intraligand LMCT d – d
6	$[Ni(L_3)(dtc)(H_2O)Cl]$	36.90(15814.6) 21.14(254.46) 15.79(110.671)	intraligand LMCT d – d
7	$[Co(L_1)(dtc)(H_2O)_2]Cl$	35.97(`22959) 31.25(12155) 20.61(712.24) 16.23(367.1) 15.57(404.01)	intraligand intraligand LMCT d – d d – d
8	$[Co(L_2)(dtc)(H_2O)Cl]$	34.72(18619.6) 30.67(1250.5) 20.83(528.64) 16.52(421.6) 15.50(293.3)	intraligand intraligand LMCT d – d d – d
9	$[Co(L_3)(dtc)(H_2O)Cl]$	37.31(21191) 25.64(1291.7) 16.26(440) 15.19(501.93)	intraligand LMCT d – d d – d
10	$[Cd\ (L_1)(dtc)(H_2O)Cl]$	34.72(32169) 28.98(44868)	intraligand LMCT
11	$Cd(L_2)(dtc)(H_2O)Cl].2H_2O$	28.98(5293.8)	LMCT
12	$[Cd(L_3)(dtc)(H_2O)_2]Cl.2H_2O$	29.23(480.8)	LMCT
13	$[Cu(L_3)(quin)(H_2O)Cl].0.5H_2O$	23.14(1828.78) 15.50(157.56)	LMCT d – d
14	$[Ni(L_1)(quin)(H_2O)_2]Cl.H_2O$	30.21(1760.84) 25.97(1231.00) 15.81(354.12)	intraligand LMCT d – d
15	$[Ni(L_2)(quin)(H_2O)Cl].0.5H_2O$	34.48(148160) 15.67(231.74)	intraligand d – d
16	$[Co(L_2)(quin)(H_2O)Cl]$	35.71(10297.7) 29.94(2089.8) 16.52(395.22) 15.15(332.86)	intraligand LMCT d – d d – d
17	$[Co(L_3)(quin)(H_2O)Cl]$	31.14(24361) 24.57(2382.43) 15.15(110.67)	intraligand LMCT d – d
18	$[Cd(L_1)(quin)(H_2O)_2]Cl$	36.36(10450.5)	intraligand

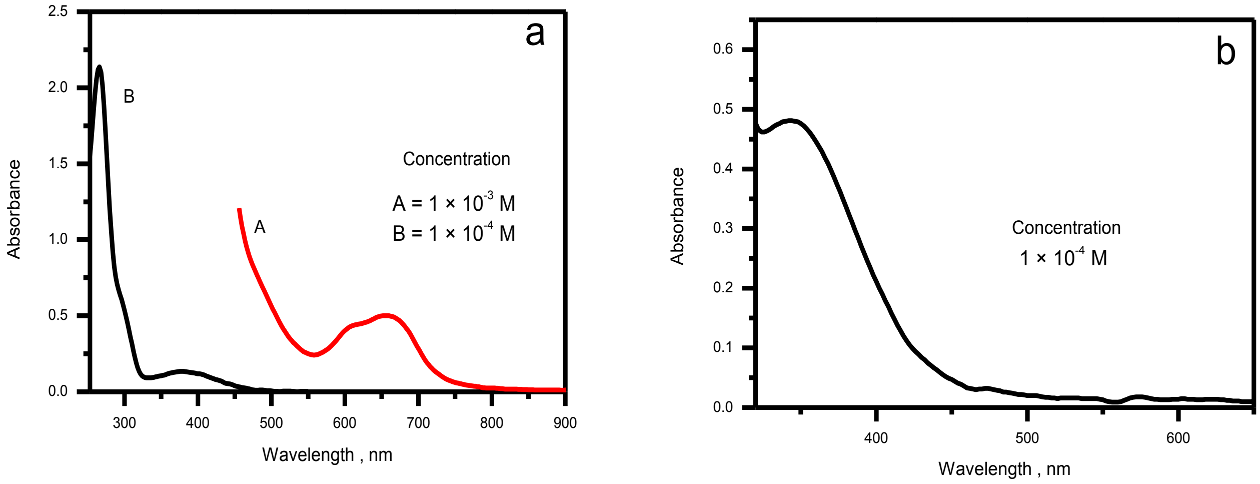

Fig. 1: Electronic spectra of the mixed ligand complexes, a = [Co(L_3)(dtc)(H_2O)Cl] and b = [Cd(L_3)(dtc)(H_2O)$_2$]Cl.2H_2O

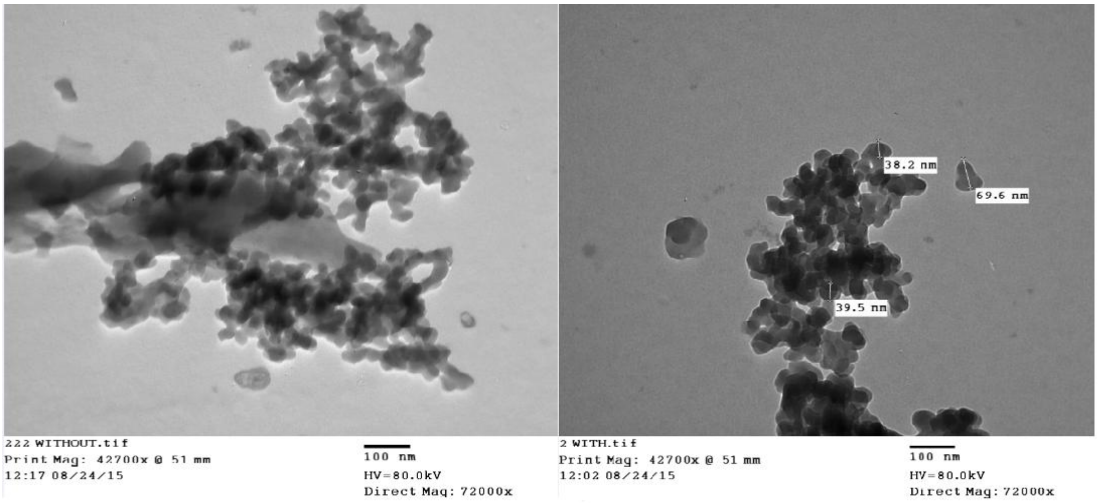

Fig. 2: TEM image of [Ni(L_3)(dtc)(H_2O)Cl] complex.

3.5. Thermal Decomposition Studies

Thermogravimetric analysis (TGA) provides a quantitative measurement of weight change *vs* temperature, and is typically used to investigate the thermal stability and compositional analysis of complexes. TGA can record directly the weight change as a function of temperature or time of transitions that involve dehydration or decomposition. Coats-Redfern and Horwitz-Metger methods were used to calculate the different kinetic parameters from thermal decomposition data [50, 51]. Thermodynamic parameters; entropy ($\Delta S^{\#}$), enthalpy ($\Delta H^{\#}$) and free energy ($\Delta G^{\#}$) of activation were calculated as shown in (Table 6) using standard relations [52]. The thermal behavior of the mixed ligand complexes 1,3 1nd 12 exhibited a mass loss on the TGA curve of 39.54, 31.81 and 31.92% (theoretical 39.88, 31.18 and 31.37%) respectively, corresponding to the loss of the hydration water molecules and start of the organic moieties decomposition (Table 5 and Fig. 4) within a temperature range 46 – 295°C.

Based on the thermal analysis data, the thermal decomposition mechanism of complex [Cu(L_3)(dtc)(H_2O)$_2$]Cl.2.5H_2O may be expressed as follows:

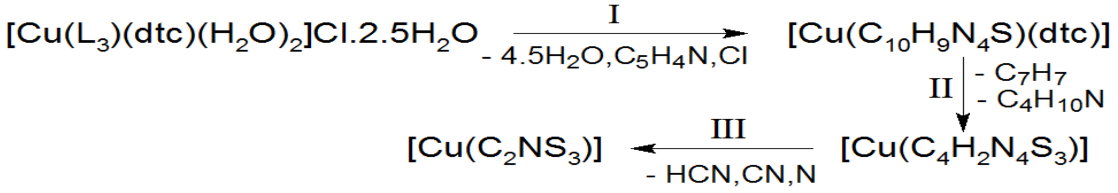

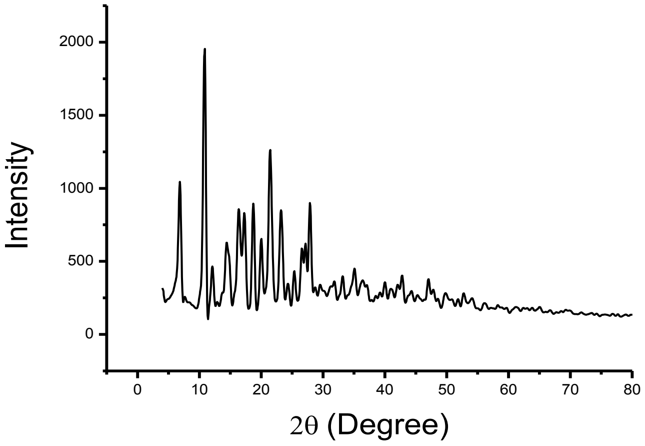

Fig.3: XRD pattern of [Ni(L_3)(dtc)(H_2O)Cl] complex

The TGA of the complex [Cu(L_3)(dtc)(H_2O)$_2$]Cl.2.5H_2O gave three steps (Fig. 4). The first step (T = 46 - 238°C, $E^{\#}$ = 59.90 kJ/mol) is assignable to the removal of four and half water molecules, C_5H_4N moiety and one chlorine atom {calcd.(found) = 31.18(31.81)%}. Step two (T = 239-370 °C, $E^{\#}$ = 73.22 kJ/mol) is assignable to removal of $C_4H_{10}N$ and C_7H_7 moieties {calcd.(found)=26.2(26.01)%}. The third step (T=372-740°C, $E^{\#}$ =26.62 kJ/mol) is assignable to removal of HCN, CN moieties and nitrogen atom {calcd.(found)=10.77(10.25)%} giving residual products as [Cu(C_2NS_3)] {calcd.(found) = 31.85(31.73)%}. The mixed ligand complexes 2, 4, 5, 11, 13, 14, and 15 lost the adsorbed and coordinated water molecules 4.67–8.35% (theoretical 4.21–8.16%) within the temperature range 45-242°C (Table 5) which corresponds to the loss of 1.5 - 3 water molecules. The thermal decomposition mechanism of complex [Cd(L_2) (dtc)(H_2O)Cl].2H_2O may be expressed as follows:

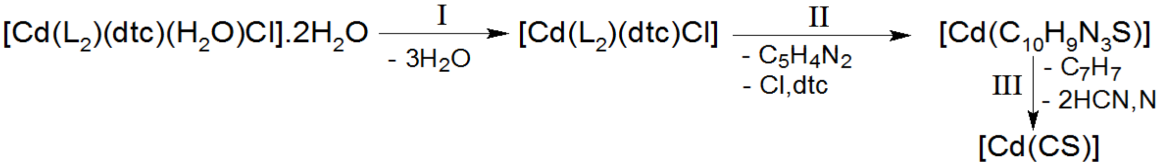

The TGA of the complex [Cd(L_2)(dtc)(H_2O)Cl].2H_2O gave three steps. The first step (T = 58 - 219°C, $E^{\#}$=27.17 kJ/mol) is assignable to the removal of three water molecules {calcd.(found) = 8.35(8.16)%}. Step two (T = 222 - 439 °C, $E^{\#}$ =58.95 kJ/mol) is assignable to removal of $C_5H_4N_2$ moiety, dtc molecule and one chlorine atom {calcd.(found) = 44.27(44.63)%}. The third step (T = 442–748 °C, $E^{\#}$ = 51.35 kJ/mol) is assignable to removal of 2HCN, C_7H_7 moieties and one nitrogen atom {calcd.(found)=24.61(24.79.)%}. Giving [Cd(CS)] as residual products {calcd.(found) = 22.77 (22.24)%}.For complexes 6 - 10 and 16 - 18, the first decomposition step represents the loss of coordinated water molecules within the temperature range of 49–239°C. Corresponding to the loss of 1–2 hydration, water molecules 2.95–6.28%(theoretical 2.77–6.18%)(Table 5 and Fig.4). The thermal decomposition mechanism of complex [Co (L_3) (Quin) (H_2O)Cl] may be expressed as follows:

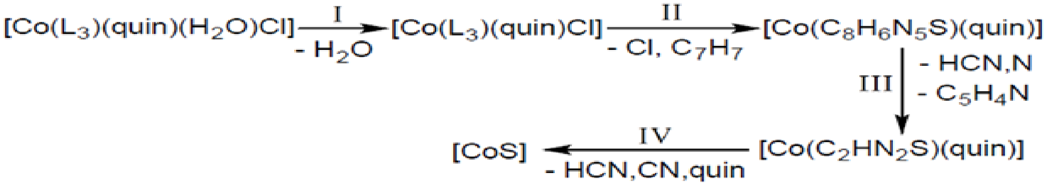

The TGA of the complex [Co(L_3)(quin)(H_2O)Cl] gave four steps (Fig. 5). The first step (T=51-151 °C, $E^{\#}$=15.91 kJ/mol) is assignable to removal of one water molecule {calcd.(found) = 3.26(3.65)%}. Step two (T=152-303°C, $E^{\#}$= 96.99kJ/mol) is assignable to removal of C_7H_7 moiety and chlorine atom {calcd.(found) = 22.86(22.36)%}. The third step (T=305-487°C, $E^{\#}$=60.68 kJ/mol) is assignable to removal of C_5H_4N, HCN moieties and nitrogen atom {calcd.(found) = 21.59(21.34)%}. The fourth step (T = 488 - 739 °C, $E^{\#}$ = 105.60 kJ/mol) is assignable to removal of quin molecule; CN and HCN moieties {calced.(found)=35.29(35.24)%}. Giving CoS as residual products {calcd.(found) = 17.00(17.12)%}.

The thermodynamic parameters; enthalpy ($\Delta H^{\#}$), entropy ($\Delta S^{\#}$) and free energy ($\Delta G^{\#}$) of activation were calculated using standard equations and the values are given in (Table 6). The ($\Delta S^{\#}$) values were found to be negative, which indicates a more ordered activated state that may be possible through the chemisorptions of decomposition products [53]. The values of activation energy for the second stage of decomposition were found to be higher than that for the first stage in complexes 1, 3 - 5, 7, 10 - 13 and 15 - 18 (Table 6) which indicates that the rate of decomposition of the second stage is lower than that of first stage, some complexes 2, 6, 8, 9 and 14 the values of activation energy for the first stage of decomposition were found to be higher than that for the second stage this may be attributed to the structural rigidity of the mixed ligands as compared with H_2O, which requires more energy for its rearrangement before undergoing any compositional change [54].

The values of the entropy for all degradation steps of all the complexes are negative. The significantly negative ($\Delta S^{\#}$) supports the assignment of an associative mechanism. However, the activation process in the studied systems seems to be strongly dominated by bond formation [55]. The positive sign of ($\Delta H^{\#}$) indicates that the decomposition stages are endothermic processes for both of them. On the other hand, the positive sign of ($\Delta G^{\#}$) reveals that all the decomposition steps are non-spontaneous.

Table 5: Thermal data for mixed ligand complexes containing diethyldithiocarbamate (dtc) ligand.

No.	complexes	steps	Temp. Range °C	Weight loss %		Loss moiety	Process	Residue	
				Calc.	Found			Calcd.(Found) %	Nature
1	$[Cu(L_1)(dtc)_2].3H_2O$	I	54-260	39.54	39.88	$3H_2O,C_5H_4N$,dtc	dehy.+decomp.		
		II	262-376	20.90	21.11	dtc	decomposition		$[Cu(C_2HN_3S)]$
		III	377-738	16.66	16.62	C_7H_7, HCN	decomposition	22.9 (22.18)	
2	$[Cu(L_2)(dtc)(H_2O)Cl].0.5H_2O$	I	57-242	4.67	4.21	1.5 H_2O	dehydration		
		II	244-371	49.91	49.28	$C_6H_5N_2$,Cl,dtc	decomposition	29.64 (30.00)	$[Cu(C_2HN_3S)]$
		III	374-746	15.77	15.46	C_7H_7	decomposition		
3	$[Cu(L_3)(dtc)(H_2O)_2]Cl.2.5H_2O$	I	46-238	31.18	31.81	$4.5H_2O,C_5H_4N$,Cl	dehy+dcomp		
		II	239-370	26.2	26.01	$C_4H_{10}N$, C_7H_7	decomposition		$[Cu(C_2NS_3)]$
		III	372-740	10.77	10.25	HCN,CN, N	decomposition	31.85(31.73)	
4	$[Ni(L_1)(dtc)(H_2O)Cl].H_2O$	I	55-189	6.29	6.03	$2H_2O$	dehydration		
		II	194-419	45.45	45.28	C_5H_4N,Cl, dtc	decomposition	32.36 (32.56)	$[Ni(C_3H_2N_4S)]$
		III	419-740	15.90	15.71	C_7H_7	decomposition		
5	$[Ni(L_2)(dtc)(H_2O)Cl].0.5H_2O$	I	47-162	4.79	4.68	$1.5H_2O$	dehydration		
		II	163-358	47.24	47.22	C_7H_7, dtc,HCN	decomposition	25.59 (25.60)	$[Ni(C_2HN_3S)]$
		III	358-741	22.38	22.30	Cl, C_6H_5N	decomposition		
6	$[Ni(L_3)(dtc)(H_2O)Cl]$	I	56-202	3.24	3.36	H_2O	dehydration		
		II	204-399	54.69	54.60	C_5H_4N,Cl, HCN $C_4H_{10}N$, C_7H_7	decomposition		$[Ni(CS)]$
		III	402-744	25.81	25.43	N,CN,CS_2,HCN	decomposition	16.26 (16.45)	
7	$[Co(L_1)(dtc)(H_2O)_2]Cl$	I	55-188	6.28	6.18	$2H_2O$	dehydration		
		II	190-294	31.43	31.42	dtc,Cl	decomposition	16.90 (16.67)	[CoS]
		III	296-731	45.39	45.73	C_5H_4N, 2HCN, C_7H_7,CN,N	decomposition		
8	$[Co(L_2)(dtc)(H_2O)Cl]$	I	47-176	3.24	3.98	H_2O	dehydration		
		II	178-289	26.66	26.97	dtc	decomposition		[Co(SCN)]
		III	290-356	22.70	22.46	Cl,C_7H_7	decomposition	20.92 (19.63)	
		IV	359-447	14.05	14.36	C_5H_4N	decomposition		
		V	450-751	12.43	12.40	2HCN, N	decomposition		
9	$[Co(L_3)(dtc)(H_2O)Cl]$	I	45-203	3.24	3.58	H_2O	dehydration		
		II	205-309	38.19	38.37	C_5H_4N,HCN, Cl,$C_4H_{10}N$	decomposition	24.34 (23.62	$[Co(CS_2)]$
		III	311-751	34.23	34.34	C_7H_7,CN,HCN, S,N	decomposition		
10	$[Cd(L_1)(dtc)(H_2O)Cl]$	I	56-108	2.95	2.77	H_2O	dehydration		
		II	110-430	45.90	45.78	C_5H_4N,dtc,2HCN	decomposition	20.65 (20.01)	$[Cd(C_3N_3S)]$
		III	433-740	20.65	20.01	C_7H_7,Cl	decomposition		
11	$[Cd(L_2)(dtc)(H_2O)Cl].2H_2O$	I	58-219	8.35	8.16	$3H_2O$	dehydration		
		II	222-439	44.27	44.63	$C_5H_4N_2$,dtc, Cl	decomposition	22.77 (22.24)	[Cd(CS)]
		III	442-748	24.61	24.79	C_7H_7, 2HCN, N	decomposition		
12	$[Cd(L_3)(dtc)(H_2O)_2]Cl.2H_2O$	I	49-295	31.92	31.37	$4H_2O$,Cl,$C_6H_5N_2$	dehy.+decmp.		
		II	295-457	22.28	22.43	dtc	decomposition	28.18 (29.02)	$[Cd(C_2HN_2S)]$
		III	458-751	17.62	17.04	C_7H_7, CN	decomposition		
13	$[Cu(L_3)(quin)(H_2O)Cl].0.5H_2O$	I	47-200	4.78	4.67	$1.5H_2O$	dehydration		
		II	202-535	42.19	42.15	C_7H_7 ,quin,HCN	decomposition		
		III	537-751	24.82	24.63	C_5H_4N, Cl	decomposition	28.21 (28.35)	$[Cu(C_3H_2N_4S)]$
14	$[Ni(L_1)(quin)(H_2O)_2]Cl.H_2O$	I	45-179	6.23	6.18	$2H_2O$	dehydration		
		II	181-355	33.61	33.32	H_2O, Cl, quin	decomposition	46.65	

	III	357-735	13.51	13.73	C_5H_4N	decomposition	(46.26)	$[Ni(C_{10}H_9N_4S)]$
15 $[Ni(L_2)(quin)(H_2O)Cl].0.5H_2O$	I	52-140	4.83	4.54	$1.5H_2O$	dehydration		
	II	141-249	6.26	6.26	Cl	decomposition		
	III	251-368	42.57	42.46	C_7H_7, quin	decomposition	32.39	$[Ni(C_3H_2N_4S)]$
	IV	370-738	13.95	13.57	C_5H_4N	decomposition	(32.86)	
16 $[Co(L_2)(quin)(H_2O)Cl]$	I	49-120	3.26	3.47	H_2O	dehydration		$[Co(C_3H_2N_4S)]$
	II	122-374	32.48	32.17	quin, Cl	decomposition		
	III	375-745	30.67	29.19	C_7H_7, C_5H_4N	decomposition	33.59(33.01)	
17 $[Co(L_3)(quin)(H_2O)Cl]$	I	51-151	3.26	3.65	H_2O	dehydration		
	II	152-303	22.86	22.36	C_7H_7, Cl	decomposition		
	III	305-487	21.59	21.34	C_5H_4N,HCN, N	decomposition	17.00(17.12)	[CoS]
	IV	488-739	35.29	35.24	quin,CN, HCN	decomposition		
18 $[Cd(L_1)(quin)(H_2O)_2]Cl$	I	54-230	5.76	5.65	$2H_2O$	dehydration		
	II	240-414	28.68	28.14	quin, Cl	decomposition		
	III	416-741	27.08	27.13	C_7H_7, C_5H_4N	decomposition	38.48(38.86)	$[Cd(C_3H_2N_4S)]$

Table 6: Thermodynamic parameters for the thermal degradation of the complexes

complexes	Steps	$E^{\#}$($kJmol^{-1}$)	$\Delta S^{\#}$ ($kJmol^{-1}K^{-1}$)	$\Delta H^{\#}$ ($kJmol^{-1}$)	$\Delta G^{\#}$ ($kJmol^{-1}$)
1 $[Cu(L_1)(dtc)_2].3H_2O$	I	29.53	-171.54	26.78	83.56
	II	47.54	-171.17	42.76	141.35
	III	113.16	-179.04	64.81	205.18
2 $[Cu(L_2)(dtc)(H_2O)Cl].0.5H_2O$	I	68.46	-161.77	64.43	142.99
	II	10.73	-122.92	6.15	73.75
	III	159.76	-151.44	154.91	243.20
3 $[Cu(L_3)(dtc)(H_2O)_2]Cl.2.5H_2O$	I	59.90	-182.20	55.56	144.33
	II	73.22	-172.30	68.46	167.06
	III	26.62	-145.20	36.09	153.31
4 $[Ni(L_1)(dtc)(H_2O)Cl].H_2O$	I	16.73	-116.71	14.05	51.74
	II	83.68	-144.06	79.15	157.66
	III	107.45	-166.42	102.00	239.01
5 $[Ni(L_2)(dtc)(H_2O)Cl].0.5H_2O$	I	11.17	-123.16	8.51	48.04
	II	35.18	-153.34	30.54	115.64
	III	104.60	-265.76	98.14	304.37
6 $[Ni(L_3)(dtc)(H_2O)Cl]$	I	56.58	-133.65	53.82	100.95
	II	24.45	-135.21	19.88	94.11
	III	24.72	-127.84	18.71	111.13
7 $[Co(L_1)(dtc)(H_2O)_2]Cl$	I	41.84	-178.17	39.11	97.72
	II	68.46	-174.16	64.08	155.86
	III	83.86	-156.43	78.69	172.55
8 $[Co(L_2)(dtc)(H_2O)Cl]$	I	55.46	-137.97	52.73	94.83
	II	20.92	-134.24	16.54	87.15
	III	13.31	-121.90	8.30	81.68
	IV	30.43	-133.25	24.78	115.25
	V	23.77	-257.31	17.53	210.51
9 $[Co(L_3)(dtc)(H_2O)Cl]$	I	27.62	-170.30	24.83	82.06
	II	16.99	-117.02	12.10	73.07
	III	41.84	-168.53	37.55	124.68
10 $[Cd(L_1)(dtc)(H_2O)Cl]$	I	14.74	-131.88	12.20	54.28
	II	125.03	-28.46	120.80	140.47
	III	29.47	-138.43	24.36	109.50
11 $[Cd(L_2)(dtc)(H_2O)Cl].2H_2O$	I	27.17	-138.77	23.27	88.35
	II	58.95	-184.86	58.95	150.58
	III	51.35	-147.97	44.30	167.78
12 $[Cd(L_3)(dtc)(H_2O)_2]Cl.2H_2O$	I	12.83	-128.11	9.71	50.45
	II	20.78	-132.48	16.35	86.83
	III	63.71	-191.28	58.65	175.14
13 $[Cu(L_3)(quin)(H_2O)Cl].0.5H_2O$	I	117.58	73.64	114.88	90.94
	II	124.57	-48.31	120.33	56.43
	III	147.39	-38.49	142.52	165.07
14 $[Ni(L_1)(quin)(H_2O)_2]Cl.H_2O$	I	56.58	-133.65	53.82	100.95
	II	24.45	-135.21	19.88	94.11

		III	20.92	-121.57	14.91	102.80
15	$[Ni(L_2)(quin)(H_2O)Cl].0.5H_2O$	I	9.2	-117.93	6.51	44.60
		II	25.67	-136.67	21.14	95.76
		III	18.06	-120.41	12.07	94.55
		IV	9.5	-111.96	2.67	94.70
16	$[Co(L_2)(quin)(H_2O)Cl]$	I	13.49	-244.14	10.70	92.48
		II	83.54	-126.11	79.40	142.33
		III	5.70	-112.89	0.9332	65.73
17	$[Co(L_3)(quin)(H_2O)Cl]$	I	15.91	-174.39	13.28	68.38
		II	96.99	-109.88	92.68	149.71
		III	60.68	-172.04	54.85	179.23
		IV	105.60	-173.90	99.35	233.01
18	$[Cd(L_1)(quin)(H_2O)_2]Cl$	I	21.63	-142.75	18.94	72.61
		II	32.06	-200.96	27.44	139.57
		III	47.54	-111.88	42.37	111.96

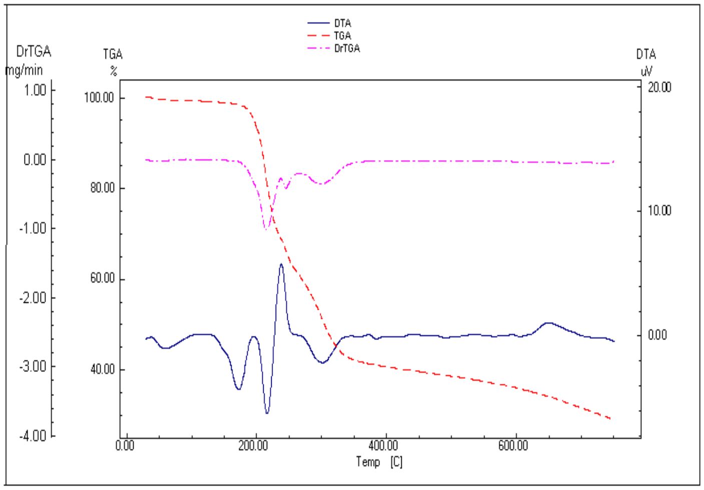

Fig. 4.TG-DTG curves of complex $[Cu(L_3)(dtc)(H_2O)_2]Cl.2.5H_2O$

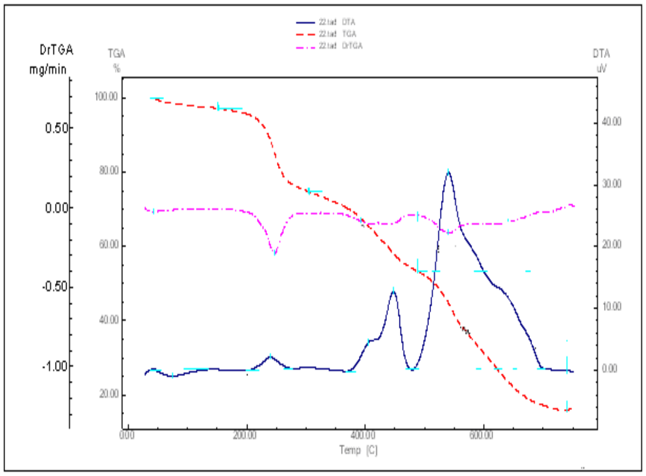

Fig. 5:TG-DTG curves of complex $[Co(L_3)(quin)(H_2O)Cl]$

3.6. Antibacterial Activity

The results of the bacteriostatic measurements are systematized in Table 7. The antibacterial studies suggested that all the synthesized materials of the metal(II) ternary complexes showed significantly enhanced antibacterial activities relative to the binary analogs. Some samples were found to be potentially active against the bacterial strains. Among them materials containing Cd(II) complexes showed enhanced activity against all bacterial strains.

Table 7: Antimicrobial activity of some binary and ternary complexes

Compound	Bacteria (Inhibition Zone in mm)					
	Staphylo-coccus aureus	*Pseudomons aerugin-osa*	*Bacillus cereus*	*Micrococcus luteus*	*Escheri-chia coli*	*Serratiamarces cens*
$[Cu(L_3)(dtc)(H_2O)_2]Cl.2.5H_2O^{(a)}$	13	14	12	17	15	16
$[Co(L_3)(dtc)(H_2O)Cl]^{(a)}$	14	12	15	13	15	17
$[Cd(L_1)(dtc)(H_2O)Cl]^{(a)}$	21	16	18	15	17	22
$[Cu(L_3)\ Cl.\ H_2O]\ Cl\ H_2O^{(b)}$	9	9	10	10	10	11
$[Co(L_3)_2Cl\ H_2O]Cl\ ^{(b)}$	10	9	10	12	10	13
$[Cd\ (L_1)Cl_2]\ 0.5H_2O^{(b)}$	12	13	13	12	13	12

$^{(a)}$ The present work, $^{(b)}$ data from reference 26

Conclusions

The ligands used in this study act as good complexing agents towards transition metal ions and they behave as symmetric bidentate ligand forming binary and ternary complexes. Nanoparticles of an average size of about 49 nm were obtained for the mixed ligand complexes prepared using soft chemistry, i.e. precipitation and filtration in normal conditions, as XRD and TEM measurements indicate. From the TG and elemental analysis data, a general formula could be established for the mixed ligands complexes involving some divalent metal ions. The TG-DTA curves provided information about the thermal stability and kinetic parameters for the thermal decomposition for these complexes

Acknowledgments-The authors are grateful for the support and facilities provided by Assiut University. M.S. Al-Salimi thanks the Yemen government for the financial support during his study in Egypt.

References

1. Milacic V., Chen D., Ronconi L., Piwowar K.R., Fregona D., Dou Q.P., *Cancer Res*., 66 (21) (2006) 10478.
2. Kaushik N. .K, Bhushand B, *Tran.Met.Chem*., 9(1984) 250.
3. Kitson T., *Chem. Educ*., 22 (1985) 43.
4. CoucouvanisD., Prog. *Inorg.Chem*. 26 (1979) 301.
5. Soroka K., Vithanage R S, Phillips D A, Walker B, Dasgupta P K, *Anal. Chem*.59 (1967) 629.
6. Mahmoud M. E., Soliman E. M., *J. Liq. Chromatogr.Rel. Technol*. 26 (2003) 3045.
7. Wen B, Shan X.Q, *Anal. Bioanal.Chem*. 374 (2002) 948.
8. Goswami A., Singh A.K., Venkataramani B, *Talanta*.60 (2003) 1141.
9. Firdaus M L, Norisuye K, Sato T, Urushihara S, Nakagawa Y, Umetani S, Sohrin Y, *Anal. Chim.Acta*. 583 (2007) 296.
10. Albrecht M, Fiege M, Osetska O, *Coord. Chem. Rev*. 252,812(2008).
11. Sengupta S K, Sahni K, Kapoor R N, Synth. React. *Inorg.Met.-Org. Chem.*, 10(1990) 269.
12. Sengupta S K, *Ind. J. Chem*., 20A (1981) 515.
13. Pandey O P, Sengupta S K and tripathi S C,*Inorg. Chim.Acta*, 90 (1394)91.
14. Srivastava V, Pandey O P, Sengupta S K, Tripathi S C, *J.Organomet. Chem.*,279(1985) 395.
15. Pandey O P, *Inorg. Chim.Acta*, 118(1956)105.
16. Blake A J, Giby L M, Gocild R O, Ppolis V I, Parsons S, Schroder M, *Acta Crystal*, C54 (1998)295.
17. Gurol I, Ashen V. and Bekergla O, *J. Chem. Soc. Dalton trans.*, (1992) 2283.
18. Furniss B S, Hannaford A J, Smith P W, Tatchell A R, *Textbook of Practical Organic Chemistry,* Vogel's (2004) 695.
19. El-Gyar S A, El-Gahami M A, El-Sameh A A, Ibrahim S A., *Polish J. Chem.* 81(2007) 1387.
20. Chidananda N, Poojary B, Sumangala V, Kumari S N, Shetty P., Arulmoli T, *Eur. J. Med. Chem.*, 51 (2012) 124.
21. Colanceska-Ragenovic V, Dimova V, Kakurinov D G, A M Buzarovska. *Molecules*, 6 (2001) 815.
22. Joshi D S, Vagdevi M H, Vaidya P V, Gadaginamath S G, *Eur. J. Med. Chem* 43 (2008) 1989.
23. Rajput S S,*Inter. J. Pharmacy and Pharm. Sci*. 4 (2012) 167.
24. Dan J, JunRui L, Chunwei X, Jiangbei M, Jianfa L, Chunyong B ,, *Bioo& Med. Chem. Lett*., 23 (2013) 1997.
25. Zhizhang L, Zheng G, Yin K, Zhang R, Deng Q, Jiannan X, *Eur. J. Med. Chem*., 44 (2009) 4716.
26. Hammam A M , EL-Gahami M A, Khafagi Z A, AL-Salimi M S, Ibrahim S A(2015)*J. Mater. Environ. Sci.* 6 (6) (2015) 1596.
27. Geary W, *Coord. Chem. Rev*, 7 (1971) 81.
28. Durgaprasad G, Sathyanarayana D N, Patel C C. *J.Chem*., 47 (1969) 631.
29. Srivastava V, Rastogi R B,*J. Inorg. Nucl.Chem*. 40 (1978) 399.
30. Criado J J, Carroco A, Macias B, Inorg.Chim.Acta, 160 (1989)31.
31. Tushar S, Basu B, Archana M, Antonin L, Eleonora R.; Robert.J, Michal H, Dick de Vos, Ulli E.*J. Organo. Chem.*, 691 (2006) 3416.
32. El-Sonbati A Z, A. El-Bindary A, Shoair A F, *Spectrochimica.Acta*. PartA, 58 (2002) 3003.
33. El-Sonbati A Z, El-Bindary A A, *New Polym. Mat*, 5 (1996) 51.
34. MohamedE. M., SawsanS. H., XarekM.A., *Polyhedron*, 28 (2009)181.

35. GuptaB. K., D. S. Gupta, S. K. Dikshit, V.Agarwala, *Ind. J. Chem.* 15A(1977) 624.
36. Subramanian M S, Viswanatha A, *J.Inorg.Nucl.Chem.*, 31(1969) 2575.
37. Kajdan T W, Squattrito P J, Dubey N S, *Inorg. Chim. Acta*. 300-302 (2000) 1082.
38. Singh G, Singh P A, Singh K, Singh D P,*Proc. Nat. Acad. Sci. Ind.* 72A (2002) 87.
39. Shukla P R, Singh V K, Jaiswal A M , Narain J,*J. Ind. Chem. Soc*. 60 (1983) 321.
40. Macias B, Villa V M, Gallego R R, *Tran. Met.Chem.*, 20 (1995) 347.
41. Boraei A AA, Synth.React.*Inorg.Met.-Org. Chem*., 32(2) (2002) 291.
42. Kishita M, Inoue M, Kubo M, *Inorg. Chem*., 3 (1964) 237.
43. Carlin R L, "*Magnetochemistry"*, Springer, Berlin, 1986.
44. Earnshow A, "*Introduction to Magnetochemistry*", Academic Press, London,1968.
45. Lever A B P, "*Inorganic Electronic Spectroscopy*" Elsevier Amsterdam, 4th, Ed, 1984.
46. Singh K, Barwa M S, Tyagi P, *Eur. J. Med. Chem*. 41(2006) 147.
47. Avaji P A, Patil S A, Badami P S, *J. Coord. Chem*. 61(2008) 1884.
48. Hambrock J, Birkner A, Fischer R A,*J. Mater. Chem.* 11 (2001) 3197.
49. El-Menyawy E M , El-Ghamaz N A , Nawar H H, J. Mol. Struct. 1036 (2013) 144.
50. Coats A W, Redfern J P, *Nature*, 20(1964) 68.
51. Horwitz H H, Metzger G, *Anal. Chem.*, 35(1963) 1464.
52. Kandil S S, El-Hefnawy B G, Baker A E, *Thermochim. Acta*, 414 (2004) 105.
53. Madhusudanan P M, Yusuff K M, Nair C G,*J. Therm. Anal.*8 (1975) 31.
54. Cotton F A, Wilkinson G,*Advanced Inorganic Chemistry*, Wiley Interscience, New York, 1988.
55. Rosic J., Petrovic B, Djuran M. I., Bugarcic Z D, *Monatsh. Chem* 138 (2007) 1.

(2017) ; http://www.jmaterenvironsci.com